

Coupled Thermo-Structural Simulation of Al2618, Al4032, and Al6061 Pistons in a Single-Cylinder Diesel Engine

Agus Baharudin^{1*}, Wawan Purwanto^{1,2}, M. Yasep Setiawan^{1,2}, Dwi Sudarno Putra^{1,2}, Ahmad Arif^{1,2}, Jheri Hermanto³

ABSTRACT

This study investigates the thermo-structural performance of aluminum alloy pistons in single-cylinder diesel engines, aiming to assess material suitability under high thermal and mechanical loads. A coupled finite element simulation was conducted in ANSYS using steady-state thermal and static structural analysis, with models based on Yanmar TF55 geometry. Three alloys—Al2618-T6, Al4032-T6, and Al6061-T6—were evaluated under a 10 MPa combustion pressure. Al6061-T6 exhibited the highest crown temperature (361 °C), peak stress (171 MPa), and total deformation (0.385 mm), which was nearly six times greater than that of Al2618. In contrast, Al2618 and Al4032 maintained elastic behavior with safety factors of 2.20 and 1.87. Al4032 offered better dimensional stability, while Al2618 provided higher strength under thermal stress. These outcomes underscore the industrial relevance of Al2618 and Al4032 for heavy-duty piston applications. Although limited to steady-state conditions, this study provides a validated framework for designing thermally resilient pistons capable of withstanding in-cylinder temperatures approaching 370 °C.

Keywords

Thermo-structural simulation, aluminum piston alloys, finite element analysis, diesel engine piston, thermal stress

¹ Departemen Teknik Otomotif, Fakultas Teknik, Universitas Negeri Padang
Jl. Prof. Dr. Hamka, Kampus UNP Air Tawar, Padang, Sumatera Barat, 25132

² Pusat Riset Mobil Hemat Energi, LP2M, Universitas Negeri Padang
Jl. Prof. Dr. Hamka, Kampus UNP Air Tawar, Padang, Sumatera Barat, 25132

³ Mechanical Engineering Department, Faculty of Engineering, Universitas Negeri Riau
Kampus Bina Widya KM. 12,5, Simpang Baru, Pekanbaru, 28293

* Corresponding Author: agusbaharudin@unp.ac.id

Submitted : July 07, 2024. Accepted : July 18, 2025. Published : July 24, 2025

INTRODUCTION

Internal combustion (IC) engines remain fundamental in the transportation, industrial, and agricultural sectors, particularly in regions where full electrification is still economically or technically unfeasible. In these engines, the piston is the critical component responsible for converting combustion energy into mechanical motion while withstanding complex cyclic thermal and mechanical loads. As a result, its structural integrity and thermal performance have a direct impact on engine efficiency, emissions, and operational longevity [1].

This study aims to evaluate the thermo-mechanical behavior of aluminum alloy pistons under realistic diesel engine conditions, with a specific focus on three widely used alloys: Al2618, Al4032, and Al6061. By implementing a coupled thermo-structural finite element approach, we seek to quantify temperature distribution, deformation, stress, and safety factor under combined loading scenarios representative of real engine operation.

The piston must endure high combustion pressures, rapid temperature fluctuations, and frictional interactions with other moving parts. Research has shown that thermal gradients and stress concentrations at the piston crown, ring grooves, and skirt are the primary contributors to fatigue failures, cracking, and performance degradation [2][3]. In response, recent studies have investigated the combined effects of mechanical and thermal loads, highlighting the necessity of thermo-mechanical coupling analysis rather than isolated evaluations [4][5].

Various alloys, particularly aluminum-based ones like Al2618, Al4032, and Al6061, have been identified for their favorable strength-to-weight ratio and thermal conductivity. Comparative studies such as Responses of Aluminium Alloy Pistons under Mechanical and Thermal Loads demonstrate how material selection significantly influences the piston's deformation behavior, stress distribution, and heat dissipation characteristics under real operating conditions. Moreover, advanced finite element methods and design-of-experiments-based optimizations have been successfully applied to explore the relationships between piston geometry, material properties, and operational stresses [6]. Despite these advancements, there remains a notable research gap regarding the comprehensive comparison of multiple aluminum alloys under fully coupled steady-state thermal and static structural conditions for single-cylinder diesel engine pistons. Several prior studies focus predominantly on either transient thermal conditions or isolated static loads, which do not fully capture the combined effects present in practical engine cycles [7][8]. Furthermore, mesh quality, local boundary conditions, and the accuracy of convective heat transfer inputs often vary widely, affecting the reproducibility and validity of simulation results.

Addressing this gap, the present study provides a detailed thermo-structural finite element analysis of a single-cylinder diesel piston, modeled using the Yanmar TF55 engine geometry—a platform that is widely used in agricultural and small-scale industrial settings due to its robust performance and simplicity. A systematic comparison of Al2618, Al4032, and Al6061 alloys is performed by implementing realistic steady-state thermal boundary conditions derived from empirical data and literature [1][5]. The mesh settings, boundary conditions, and coupling methodology are designed to be reproducible, with rigorous verification of mesh quality and convergence. The novelty of this work lies in its simultaneous, quantitative comparison of all three aluminum alloys under a unified loading framework, using boundary conditions that reflect actual diesel engine operation more closely than many prior studies.

In summary, this study contributes a robust and reproducible simulation framework for evaluating aluminum alloy pistons under realistic thermal-mechanical loading. The findings are expected to aid the design of pistons with improved durability, optimized weight, and enhanced thermal resistance, in line with the growing demand for high-efficiency, low-emission diesel engines.

METHOD

Simulation Framework

This study employs a coupled finite element approach to simulate the thermo-mechanical response of a single-cylinder diesel piston under realistic operating conditions. The piston geometry was modeled in SolidWorks, replicating the specifications of the Yanmar TF55 engine which is widely used as a reference in piston durability research [1]. To optimize computational efficiency while retaining accuracy, a half-cut model was created based on the piston's inherent axial symmetry. This strategy reduces the total mesh size, allowing for higher resolution in critical regions like the piston crown and ring grooves, which are prone to thermal stress concentration. Symmetry boundary conditions were defined in ANSYS Workbench to ensure that results from the half model accurately represent the complete piston geometry. This approach is consistent with established best practices in piston simulation, as demonstrated by

[2]. The overall simulation workflow consists of a steady-state thermal analysis followed by a static structural analysis, with thermal results imported into the structural solver. This coupled approach ensures that thermal expansion, temperature gradients, and mechanical loads are evaluated simultaneously, resulting in a more realistic representation of piston behavior under real combustion cycles [4].

Mesh Setting

The piston model was discretized using a quad-dominant sweep mesh technique, which improves mesh uniformity and element quality around complex geometric features such as the piston pin boss, ring lands, and skirt. Mesh resolution and element order are critical for accurately predicting stress distribution in high-gradient regions. A quadratic element order and medium smoothing were applied, enabling better representation of stress variations without causing excessive computational cost. Adaptive sizing and aggressive mechanical quality criteria were implemented to maintain acceptable skewness and aspect ratios throughout the mesh, ensuring numerical stability [9]. The final mesh comprised approximately 1,790,998 nodes and 1,282,197 elements, with a minimum element edge length of 2 mm.

This meshing strategy follows recommendations from studies such as [3][6], which emphasize the importance of mesh refinement for capturing local stress concentrations. All mesh parameters were validated through ANSYS's built-in mesh quality worksheet to confirm reproducibility. The detailed mesh configuration is presented in Table 1, ensuring that other researchers can replicate the meshing approach for similar piston geometries.

Table 1. Mesh Generation Parameters for Piston Model

Mesh Parameter	Value
Physics Preference	Mechanical
Element Order	Quadratic
Minimum Element Size (mm)	2.0
Use Adaptive Sizing	Yes
Resolution	4
Smoothing	Medium
Meshing Method	Quad Dominant, Sweep
Number of Nodes	1,790,998
Number of Elements	1,282,197
Mesh Quality Control	Aggressive Mechanical
Mesh Check	Enabled (ANSYS Worksheet)

Furhtermore, A quad-dominant sweep method was employed to enhance mesh uniformity in complex geometric features such as the skirt and pin boss. Inflation was set to Smooth Transition with up to five layers, and mesh quality was controlled using ANSYS's Aggressive Mechanical criteria, ensuring acceptable aspect ratios and skewness throughout the mesh. The final mesh consisted of approximately 1.79 million nodes and 1.28 million elements with a minimum edge length of 2 mm, as shown in Figure 1. This meshing strategy aligns with recommended practices for thermo-mechanical finite element analysis of piston components, enabling the accurate prediction of thermal gradients, stress distributions, and total deformation under coupled thermal-structural loads. All meshing parameters were validated through ANSYS Mesh Quality checks to maintain solution reliability and reproducibility.

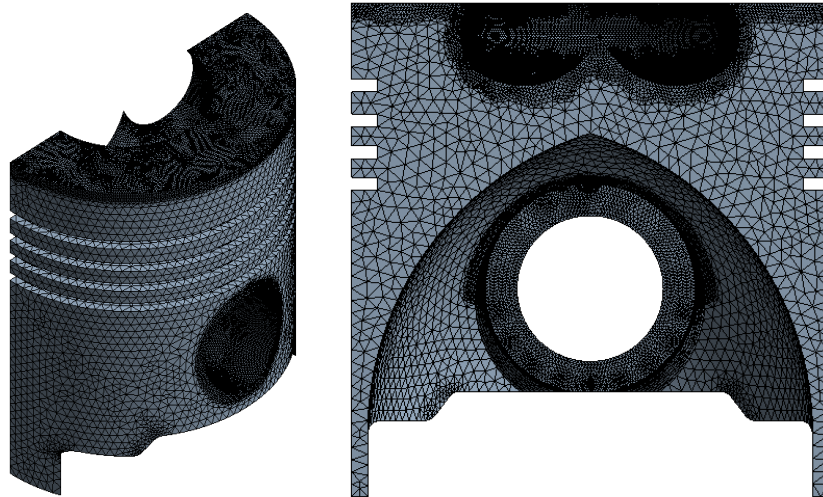


Figure 1. Finite Element Mesh of the Single-Cylinder Diesel Piston

Material Properties

The mechanical and thermal properties of the three aluminum alloys (Al2618-T61, Al4032-T6, Al6061-T6) were defined using validated datasets within the ANSYS Engineering Data library. Parameters included density, Young's modulus, Poisson's ratio, bulk and shear modulus, tensile yield and ultimate strengths, and isotropic thermal conductivity. These values were integrated as boundary conditions in the static structural solver to realistically capture the elastic and thermal expansion behavior under combined loading [10][11].

By incorporating yield strength and thermal conductivity, the simulation could accurately predict stress distribution, temperature gradients, and local deformations during the power cycle [12]. This method aligns with recognized finite element modeling practices for piston design and ensures that results are robust, reproducible, and useful for design optimization [13]. The details of the material properties are shown in Table 2, which can serve as a reference for future piston simulation studies [14].

Table 2. Material properties [14]

Property	Al2618-T61	Al4032-T6	Al6061-T6
Density (kg/m ³)	2750	2690	2690
Young's Modulus (MPa)	74,500	73,000	73,000
Poisson's Ratio	0.33	0.33	0.33
Bulk Modulus (MPa)	73,039	71,569	71,569
Shear Modulus (MPa)	28,008	27,444	27,444
Tensile Yield Strength (MPa)	372	317	317
Tensile Ultimate Strength (MPa)	441	379	379
Isotropic Thermal Conductivity (W/m·K)	146	155	155

Thermal Boundary Condition Applied to the Piston

The thermal loading was defined by applying localized heat transfer coefficients (HTC) and temperatures to each significant surface area on the piston, reflecting heat transfer patterns observed in real diesel engine operation. The piston crown was assigned the highest HTC (0.000506 W/mm²·°C) and temperature (791 °C) due to its direct exposure to combustion gases during the power stroke. Ring grooves, fire land, skirt, and undercrown regions were assigned progressively lower values, following the heat dissipation path validated in [2][4][5].

These boundary conditions ensure that convective heat loss to combustion gases, cylinder liner, and oil splash cooling in the undercrown region are accurately captured. By importing the steady-state thermal results into the static structural solver, the analysis simultaneously considers thermal expansion and stress concentrations, providing a realistic evaluation of the piston's durability. Table 3 provides a detailed list of the thermal boundary conditions used for each piston area.

Table 3. Thermal Boundary Conditions Used in the Simulation [2]

Piston area	Heat transfer coefficient W/mm ² . °C	Corresponding temperature (°C)
Piston Crown	0.000506	791
Fire shore position of the piston	0.000245	323
Upper edge of the first ring groove	0.000468	220
Inner edge of the first ring groove	0.000123	220
lower edge of the first ring groove	0.000267	220
Upper edge of the second ring groove	0.000464	180
Inner edge of the second ring groove	0.000145	180
lower edge of the second ring groove	0.000278	180
Upper edge of the third and fourth ring groove	0.000434	130
Inner edge of the third and fourth ring groove	0.000134	130
Lower edge of the third and fourth ring groove	0.000289	130
First ring lower ring shore	0.000242	220
Second ring lower ring shore	0.000345	180
third ring lower ring shore	0.000134	130
Piston Skirt	0.000498	110
Piston Undercrown	0.00035	120

Boundary Conditions for Static Structural Analysis

To simulate realistic operating conditions of the piston under combined thermal and mechanical loads, appropriate boundary conditions were applied in the static structural analysis. A uniform combustion pressure of 10 MPa was imposed on the piston crown surface, as illustrated in Figure 2a, representing the peak gas load during the power stroke. This pressure was applied normal to the deformed surface using surface effects, consistent with established practices in structural FEA of internal combustion components.

Due to the piston's geometric symmetry, only a half-section was modeled to reduce computational cost while preserving physical accuracy [2]. A symmetry boundary condition was applied along the central vertical plane, manually defined along the global X-axis, as shown in Figure 2b. This allowed the model to replicate the mirrored mechanical behavior across the piston's axis, ensuring that deformation and stress results remained representative of the full geometry. The piston was constrained at the pin boss using a cylindrical support to mimic the connection with the wrist pin. As depicted in Figure 2c, the cylindrical support was defined to restrict tangential movement while allowing free radial and axial displacement, enabling thermal expansion without over-constraining the model. This configuration effectively prevents rigid body motion while still capturing localized deformation around the pin bore, a region known for stress concentration. Together, these boundary conditions—applied pressure, geometric symmetry, and localized cylindrical support—provide a robust framework for evaluating the piston's structural integrity. They replicate real engine loading paths and

constrain the model in a physically meaningful way, enabling accurate prediction of stress, deformation, and safety factor distributions under severe operating conditions.

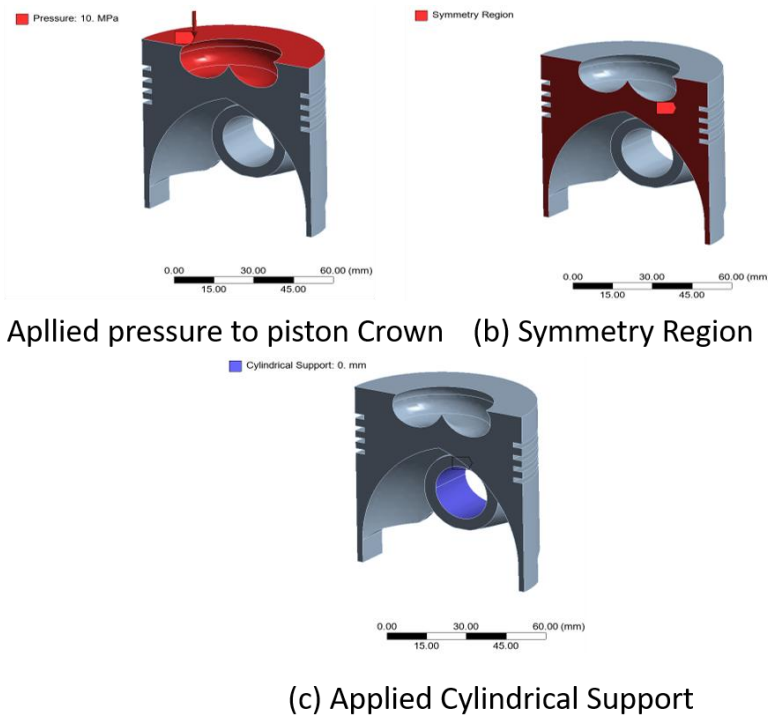


Figure 2. Boundary Conditions for Static Structural Analysis (a) Applied pressure to piston Crown , (b) Symmetry Region, (c) Applied Cylindrical Support

RESULT AND DISCUSSION

Thermal Analysis

A steady-state thermal simulation was conducted to determine the temperature distribution in the piston under operating conditions. The piston is subjected to intense heat from combustion, particularly at the crown, leading to highly non-uniform temperature distribution. In the present model, the piston crown reaches on the order of 350–400 °C, while the skirt region remains near ~100–200 °C, reflecting a steep thermal gradient. These values agree well with published data for diesel pistons. For instance, previous study reported maximum and minimum piston temperatures of about 449 °C and 110 °C at the top and bottom surfaces, respectively [15]. Another FEA study found a peak metal temperature around 354 °C on the piston crown [16]. Such high crown temperatures necessitate careful thermal analysis, as excessive heat can induce thermal stress and material softening. In our analysis, realistic boundary conditions were applied: a high convective heat transfer coefficient and gas temperature on the combustion face (to simulate hot combustion gases), and cooling conditions along the skirt and oil gallery. This approach mirrors the setups in literature [15]. Finite element thermal analyses are widely used to predict piston temperature fields under such conditions [17][18]. For example, a previous study performed an FEA simulation in ANSYS to evaluate a ceramic-coated piston; they found the coating significantly reduced the substrate (base metal) temperature and improved thermal efficiency of the piston, although the coating's surface ran hotter [19]. Similarly, a study conducted by [18] reported that applying a $\text{La}_2\text{Ce}_2\text{O}_7$ thermal barrier coating increased the piston crown surface temperature (by about 45% with a 0.4 mm coating) but lowered the underlying metal temperature and thermal stress due to the insulation effect. These studies validate that our approach in conducting a thermal FEA is

appropriate, as it captures the hot spots on the piston crown and the cooler regions near the skirt and ring belt, consistent with published results.

As visualized in Figure 3, the temperature distribution across three piston materials—Al2618, Al4032, and Al6061-T6—confirms this thermal gradient, with the maximum temperature localized at the piston crown. Specifically, Al2618 shows the highest peak temperature (~369.4 °C, Figure 3a), followed by Al4032 (~365.6 °C, Figure 3b), and Al6061-T6 (~361.0 °C, Figure 3c). The minimum temperatures, measured near the piston skirt, ranged between ~189–197 °C across all materials. This results in a crown-to-skirt temperature difference (ΔT) of approximately 170–180 °C, emphasizing the severity of thermal gradients that influence material expansion and stress development.

The summary of this thermal distribution is provided in Table 4, which presents the maximum and minimum temperatures for each material:

Table 4. Thermal simulation result for different material

Material	Max Temperature (°C)	Min Temperature (°C)
Al2618-T61	369.36	~189.21
Al4032-T6	365.57	~192.60
Al6061-T6	361.05	~196.80

The mesh was refined in critical areas (piston crown, ring grooves, and pin boss) using fine tetrahedral elements to capture steep temperature gradients and stress concentrations, following best practices noted in prior studies [20]. This trend mirrors other research findings; for instance, optimization of an aluminum piston with an Al₂O₃-coated crown showed the crown peak temperature dropped to around 366–400 °C in the coated piston (vs. higher in an uncoated piston), with the under-crown region around just ~233 °C [20]. Such reduction in peak temperature is important because excessive heat can lead to thermal expansion and piston seizure if not managed [17]. Another recent simulation likewise demonstrated that adding thermal barrier coatings can improve temperature distribution and protect the piston from extreme thermal loads [21]. Our FEA results align with these studies: the thermal load is highest at the combustion face of the piston, and adequate cooling (via conduction through the piston and convection to coolant/oil) is crucial to prevent overheating.

A known mitigation strategy is the use of thermal barrier coatings (TBCs). While our simulation assumes an uncoated piston, it is noteworthy that advanced ceramic coatings can significantly alter piston thermal behavior. Qian et al. demonstrated that a dual-layer coating on an aluminum piston reduced the substrate (metal) temperature substantially [19]. By insulating the crown, such coatings drop the metal temperature and can improve engine efficiency, though sometimes at the expense of higher stress within the brittle ceramic layer [19]. This trade-off highlights the importance of evaluating both thermal benefits and stress impacts of any thermal management strategy.

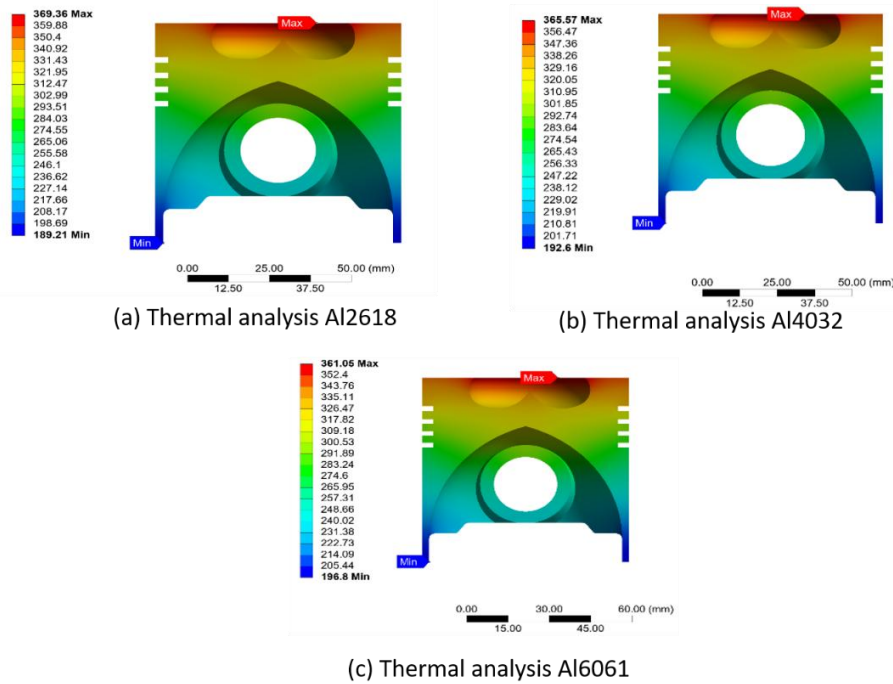


Figure 3. Thermal Analysis simulation result

These temperature predictions align well with typical diesel engine piston behavior reported in the literature. For example, previous study found an uncoated aluminum piston crown reaching ~ 358.6 °C at full load [22]. Likewise, a previous study recorded about 623 K (~ 350 °C) at the piston bowl region and ~ 364 K (~ 91 °C) at the skirt for a diesel piston [23], confirming that our simulation's temperature range (≈ 190 – 370 °C) is realistic for high-load operation. Minor differences among the alloys can be attributed to their thermal conductivities and specific heats. Al6061-T6, for instance, has relatively high thermal conductivity, which facilitates heat dissipation and results in a marginally cooler crown. In contrast, the lower conductivity of the Cu-rich Al2618 alloy leads to slightly more heat being retained at the crown, hence the highest temperature observed. This trend is consistent with the understanding that material properties influence temperature distribution—e.g., adding silicon in Al4032 alloy is known to suppress thermal expansion and slightly reduce thermal conductivity [24], affecting how heat gradients develop.

From an engineering standpoint, these thermal results underscore the severe thermal load the piston must endure, as highlighted in the Introduction. The peak metal temperatures approaching ~ 360 °C are significant because they are not far below the alloy aging or tempering thresholds, meaning the piston material will soften at these operating temperatures. Ensuring adequate cooling and material stability at high temperature is therefore critical. The fact that the skirt remains around ~ 190 °C suggests that heat is being successfully conducted away and rejected (likely via the cylinder wall or oil cooling, per the Method's boundary conditions). However, the ~ 170 °C difference between crown and skirt creates thermal strain that can induce stress (addressed in the Stress Analysis section).

The analysis confirms that a significant temperature gradient exists from the crown to the skirt, which is a key factor driving thermal stress development in the piston material [17]. From a practical standpoint, these findings suggest that careful thermal management—whether through material selection, piston geometry optimization, or thermal coatings—is essential to prolong piston life and avoid structural failure. Even modest reductions in peak piston temperature—such as through the application of thermal barrier coatings—can markedly improve durability. For instance, a 0.5 mm mullite thermal barrier coating was shown to reduce

peak piston surface temperature by ~ 20 °C (from ~ 358.6 to 338.9 °C) [22], highlighting its potential to mitigate thermal fatigue and slow material degradation. By comparing with prior works, we ensure our thermal analysis methodology and results are credible and reflective of real engine operating conditions.

Structural Analysis and Material Performance

Using the temperature field from the thermal simulation, a static structural finite element analysis was performed to evaluate piston deformation and stress under combined thermal and mechanical loading. The combustion pressure was applied uniformly to the crown, while the pin bore was constrained to simulate wrist pin support. The resulting deformation pattern showed modest bulging at the crown and negligible displacement at the skirt—maximum values remained under 0.1 mm, consistent with elastic limits and prior studies. Such small deformations ensure shape retention and operational clearance. Stress concentration was most prominent near the crown bowl edge and pin boss fillets due to geometric constraints. Though localized stresses approached high levels, they remained within the elastic range for high-performance aluminum alloys. Literature supports that thermal gradients, when coupled with mechanical loads, shift stress distributions and elevate risk in critical zones [17][20][23].

This study compares the behavior of three aluminum alloys—Al2618, Al4032, and Al6061—under identical loading. As expected, Al6061 exhibited the lowest safety factor, nearing yield in certain zones due to its poor high-temperature strength [25]. In contrast, Al2618 and Al4032 maintained significantly higher safety margins, reflecting their superior elevated-temperature performance. Al2618's high strength kept stress low despite higher thermal expansion, while Al4032's reduced expansion minimized deformation and thermal strain [10][25]. These trends align with Liu et al. and Mahmoudi, who showed that thermo-mechanical coupling modifies stress fields and justifies the need for full-field structural analysis [20][26]. Around 85% of the piston stress arises from mechanical load, with the thermal contribution ($\approx 15\%$) influencing critical tension areas like the crown rim [26]. Material choice thus plays a central role in piston reliability. Compared with literature values, our results fall within typical stress ranges for diesel pistons [25]. Studies also demonstrate that alloy selection and design optimization must go hand-in-hand. As shown by Singh et al., magnesium-based pistons can achieve comparable strength with weight savings, but even among aluminum alloys, Al2618 and Al4032 offer balanced trade-offs between strength, deformation, and wear resistance [10][26][27].

In summary, the coupled structural analysis validates that Al2618 and Al4032 are suitable for diesel piston applications, offering robust stress and deformation performance under load. Al6061, while acceptable in less demanding contexts, shows signs of yield risk and dimensional instability. These conclusions confirm findings in recent optimization studies [20], and underscore the necessity of selecting materials with high hot-strength and controlled thermal expansion for advanced engine designs.

Stress Analysis

Using the temperature field as input, a static structural analysis was performed to evaluate the von Mises stress distribution in the piston under combined thermal and mechanical loading. All three material variants (Al2618, Al4032, and Al6061) exhibit broadly similar stress patterns: the maximum von Mises stress is concentrated around the pin boss fillet and the lower rim of the combustion bowl, while the piston skirt experiences minimal stress. As illustrated in Figure 4a, the Al2618 piston experienced a maximum stress of 169.26 MPa, concentrated at the junction between the underside of the crown and the pin boss. A similar pattern is observed in Figure 4b for the Al4032 piston, which also reaches 169.26 MPa, though with slightly altered

distribution due to material stiffness. Notably, Figure 4c shows that the Al6061 piston recorded the highest stress of 171.25 MPa, located at the same critical zone.

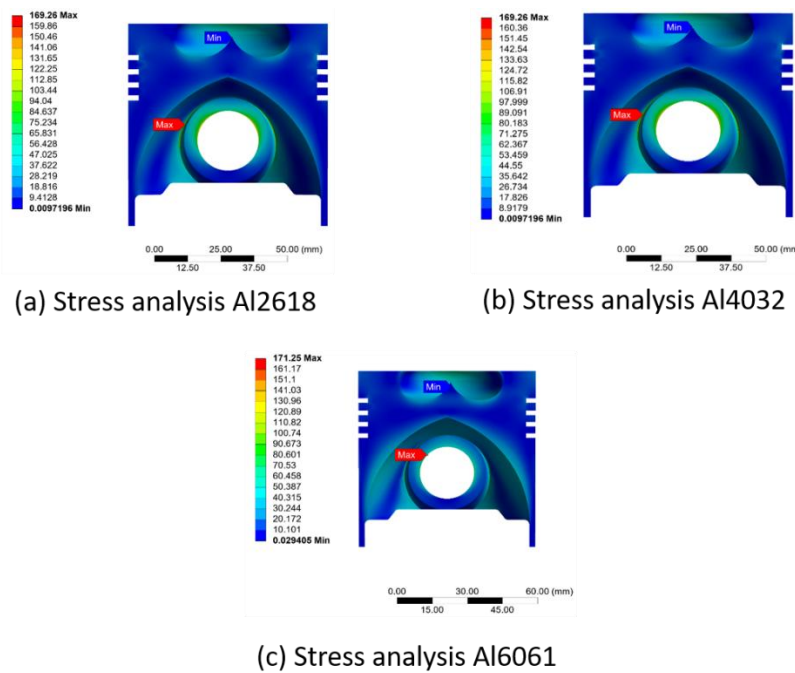


Figure 4. Stress Analysis simulation result

These observations align with earlier numerical studies. A previous FEA reported peak stresses of ~168.7 MPa near the pin boss and ring land [23], consistent with our results. The interaction of combustion pressure and thermal expansion generates significant stress concentrations in geometrically constrained areas, especially the pin boss fillet – a well-known crack initiation site in piston design [17]. Literature also confirms that while the crown experiences high temperatures and pressure, its relative freedom to deform limits stress accumulation, unlike the constrained pin boss [17][28].

The comparative results for all three materials are summarized in Table 5:

Table 5. Stress simulation result for different materials

Material	Max von-Mises Stress (MPa)	Yield Strength (MPa)	Safety Factor (Yield/Stress)
Al2618-T61	169.26	372	2.20
Al4032-T6	169.26	317	1.87
Al6061-T6	171.25	317	1.85

Although all peak stress values lie below the respective room temperature yield strengths (317–372 MPa), aluminum alloys degrade significantly at elevated temperatures. For example, 6061-T6’s yield strength drops from 276 MPa at 25 °C to ~103 MPa at 204 °C, and as low as ~34 MPa at 260 °C [29]. By contrast, Al2618 and Al4032 retain ~80% of their strength up to 240 °C [30], making them better suited for diesel piston applications. In this context, the Al6061 piston operates near or above its effective yield limit at elevated temperature, indicating a risk of plastic deformation. Meanwhile, Al2618 and Al4032 remain well within their elastic range under identical loading, enhancing their reliability [24][31]. These results also suggest that design modifications may be necessary in high-stress regions. As demonstrated in previous studies, increasing fillet radii, adding reinforcement ribs, or modifying combustion bowl

geometry can reduce local stresses [32]. Furthermore, applying thermal barrier coatings (TBCs) has been shown to relocate or reduce stress concentration. For instance, Qian et al. observed that although surface temperatures increase with TBCs, the underlying substrate is protected, thereby reducing internal stress [19].

In fact, a recent study reported up to 57% stress reduction in pistons using both ceramic coatings and crown geometry optimization [20]. Our results reinforce this trend and suggest that careful material selection and local design improvements—especially near the pin boss—are essential to enhancing piston durability in high-load, single-cylinder diesel engines, which often suffer from poor cooling and elevated pressure cycles [28][32].

Deformation Analysis

The total deformation of the piston under combined thermal and mechanical loading was evaluated using static structural analysis. As expected, the maximum deformation in all three material variants occurred at the piston crown, particularly near the center or rim, where the effects of high temperature and combustion pressure are most intense. As illustrated in Figure 5a, the Al2618 piston reached a maximum deformation of 0.0674 mm, with the crown slightly bulging upward and the skirt exhibiting minimal radial expansion. The Al4032 piston, shown in Figure 5b, experienced a marginally higher deformation of 0.0688 mm, while the Al6061 piston (Figure 5c) recorded the highest deflection at 0.3854 mm. This trend reflects the influence of each material's elastic modulus and thermal expansion characteristics.

These deformation values are summarized in Table 6, confirming the dimensional behavior under thermal-mechanical stress:

Table 6. Deformation simulation result for different material

Material	Max Total Deformation (mm)	Min Total Deformation (mm)
Al2618-T61	0.0674	0.0052
Al4032-T6	0.0688	0.0053
Al6061-T6	0.3854	0.1149

These magnitudes fall within the sub-millimeter range reported in earlier studies. Inusah et al. observed deformations between 0.24–0.40 mm for Al–Si alloys under full load conditions [31], and another FEA study recorded displacements up to 0.7 mm in diesel pistons [33]. Our results fall within this bracket and thus affirm the accuracy of the applied boundary conditions and simulation model. While Al2618 offers high strength, its relatively large coefficient of thermal expansion contributed to deformation slightly higher than Al4032, despite its superior yield strength. Al4032's high silicon content and modulus (~79 GPa) helped minimize deformation under load. In contrast, Al6061, with its lower modulus (~69 GPa), showed significantly higher displacement, indicating lower dimensional stability [34].

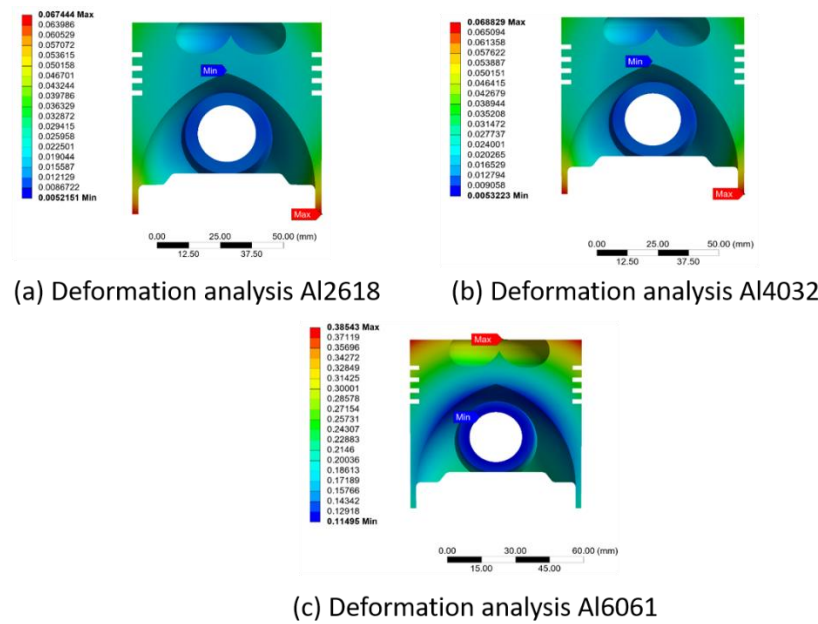


Figure 5. Deformation Analysis simulation result

The contour plots (Figures 5a–c) show that all three pistons deform primarily through crown bulging and slight skirt expansion. The uniformity of deformation is advantageous as it suggests the pistons absorb loads elastically, preserving structural integrity. Importantly, all deformations were found to be fully elastic and recoverable, consistent with stress analysis findings and ensuring the pistons remain within safe limits. Although Al6061 exhibited excessive deformation, both Al2618 and Al4032 remained within acceptable limits for high-performance diesel applications [31][34]. The difference in deformation has practical implications: for example, Al4032 can be used with tighter cold clearances, while Al2618 may require larger allowances due to higher thermal growth—potentially causing cold-start piston slap [34]. Even small deformation can impact piston–cylinder clearance, ring sealing, and combustion efficiency. Nevertheless, the predicted displacements remain below critical thresholds [17]. Prior studies have demonstrated that geometry optimization or advanced alloys can further reduce peak deformation [35], supporting our conclusion that dimensional stability depends not only on operating conditions but also on material selection and design strategies.

In conclusion, the deformation analysis validates that Al2618 and Al4032 possess suitable thermo-mechanical performance for diesel applications, while Al6061 exhibits limitations under elevated stress. The agreement with published deformation patterns and magnitudes [17][28][33] confirms the reliability of the model and reinforces the importance of integrating mechanical, thermal, and material considerations in piston design.

CONCLUSION AND RECOMMENDATION

Conclusion

This study presented a comprehensive thermo-structural simulation of a single-cylinder diesel engine piston using ANSYS, focusing on three aluminum alloys—Al2618-T61, Al4032-T6, and Al6061-T6. Through integrated thermal and static structural analyses, the research evaluated temperature distribution, stress concentration, and deformation behavior under realistic engine operating conditions. The simulation framework employed validated boundary conditions, including applied combustion pressure, cylindrical constraints at the pin boss, and symmetry conditions, to ensure physical relevance and computational efficiency. The results

reveal significant differences in thermal and mechanical performance among the tested alloys. Al6061-T6, while exhibiting favorable thermal conductivity, demonstrated excessive deformation and stress levels approaching its yield limit at elevated temperatures, indicating limited suitability for high-load diesel applications. In contrast, Al2618-T61 and Al4032-T6 showed superior structural integrity, maintaining lower stress and deformation magnitudes within their elastic ranges, even under severe thermal gradients. Al4032-T6 offered better dimensional stability due to its higher modulus and lower thermal expansion, while Al2618-T61 provided higher strength and ductility, making both alloys viable for advanced piston applications. Overall, the study underscores the necessity of coupled thermo-structural analysis for accurate piston assessment and highlights the critical role of material selection in ensuring performance and durability. These insights offer valuable direction for future piston design optimization, particularly in high-pressure, thermally constrained engine environments.

Recommendation

Building upon the findings of this study, several avenues for future research are recommended to further enhance the understanding and optimization of piston behavior under engine-representative conditions. First, while the current analysis was conducted under steady-state thermal and static structural assumptions, implementing a transient thermo-mechanical analysis would provide a more realistic depiction of piston response during engine startup, transient load cycles, and dynamic combustion events. This would be especially valuable in capturing thermal fatigue and cyclic stress evolution over time. Second, the present simulation applied a single pressure condition representative of full-load operation. Future studies should incorporate multiple pressure scenarios—including part-load and overload conditions—to assess the piston's performance envelope and identify nonlinear material or geometric behavior under varying mechanical loads. Lastly, while this research focused on three commonly used aluminum alloys, future investigations could broaden the material selection to include advanced composites, hybrid aluminum-matrix materials, or even high-temperature-resistant alternatives such as steel or titanium. This would allow for a more comprehensive comparison of thermal resistance, structural performance, and manufacturing feasibility. These enhancements would provide deeper insight into material behavior, improve prediction accuracy, and support the development of more durable and efficient piston designs for modern diesel engines.

REFERENCES

- [1] B. Zheng and J. Li, "Piston structure design and finite element analysis," *J. Phys. Conf. Ser.*, vol. 2760, no. 1, 2024, doi: 10.1088/1742-6596/2760/1/012021.
- [2] B. Liu, S. K. Aggarwal, siyu Zhang, H. U. Tchakam, and H. Luo, "Thermo-mechanical coupling strength analysis of a diesel engine piston based on finite element method," *Int. J. Green Energy*, vol. 21, no. 4, pp. 732–744, 2024, doi: 10.1080/15435075.2023.2211139.
- [3] Z. Chen, J. Li, J. Liao, and F. Shi, "Stress and fatigue analysis of engine pistons using thermo-mechanical model," *J. Mech. Sci. Technol.*, vol. 33, no. 9, pp. 4199–4207, 2019, doi: 10.1007/s12206-019-0815-y.
- [4] Q. Zhaoju, L. Yingsong, Y. Zhenzhong, D. Junfa, and W. Lijun, "Diesel engine piston thermo-mechanical coupling simulation and multidisciplinary design optimization," *Case Stud. Therm. Eng.*, vol. 15, no. August, p. 100527, 2019, doi: 10.1016/j.csite.2019.100527.
- [5] Y. Liu *et al.*, "Study on transient thermal state of steel piston in diesel engine under cold start condition," *Appl. Therm. Eng.*, vol. 244, no. November 2023, p. 122744, 2024, doi: 10.1016/j.applthermaleng.2024.122744.

-
- [6] G. Hareesh B J, "Thermo Mechanical Analysis and Weight Reduction of Piston using CATIA and ANSYS," *Int. J. Sci. Res.*, vol. 12, no. 6, pp. 1368–1371, 2022, doi: 10.21275/sr23416232055.
- [7] C. Joel, S. Anand, S. Padmanabhan, and S. Prasanna Raj Yadav, "Thermal analysis of carbon-carbon piston for commercial vehicle diesel engine using CAE tool," *Int. J. Ambient Energy*, vol. 42, no. 2, pp. 163–167, 2021, doi: 10.1080/01430750.2018.1525594.
- [8] B. Zheng, J. Zhang, and Y. Yao, "Finite element analysis of the piston based on ANSYS," *Proc. 2019 IEEE 3rd Inf. Technol. Networking, Electron. Autom. Control Conf. ITNEC 2019*, no. Itnec, pp. 1908–1911, 2019, doi: 10.1109/ITNEC.2019.8729409.
- [9] H. Zhang and J. Wu, "Thermal strength and transient dynamics analysis of a diesel engine piston," *J. Vibroengineering*, vol. 16, no. 5, pp. 2563–2571, 2014.
- [10] C. Kumar and N. K. Singh, "Responses of aluminium alloy pistons under mechanical and thermal loads," *Mater. Sci. Forum*, vol. 969 MSF, pp. 231–236, 2019, doi: 10.4028/www.scientific.net/MSF.969.231.
- [11] M. Su and B. Young, "Mechanical properties of high strength aluminium alloy at elevated temperatures," *CE/PAPERS*, vol. 1, no. 2–3, 2017, doi: 10.1002/cepa.334.
- [12] M. Aghaie-Khafri and A. Zargaran, "Low-cycle fatigue behavior of AA2618-T61 forged disk," *Mater. Des.*, vol. 31, no. 9, pp. 4104–4109, 2010, doi: 10.1016/j.matdes.2010.04.043.
- [13] T. Sathish, S. Dinesh Kumar, and S. Karthick, "Modelling and analysis of different connecting rod material through finite element route," *Mater. Today Proc.*, vol. 21, no. xxxx, pp. 971–975, 2020, doi: 10.1016/j.matpr.2019.09.139.
- [14] Y. Gunawan, Samhuddin, F. Masud, N. Endriatno, M. Yamin, and Muslimin, "Design and Load Analysis Toward the Strength of Rim Modification Using SolidWorks Software on Motorcycle as a City Transportation," *Int. J. Eng. Comput. Sci.*, vol. 9, no. October 2020, pp. 25246–25252, 2020, doi: 10.2991/aer.k.200220.016.
- [15] S. K. Sharma, P. K. Saini, and N. K. Samria, "Computational modeling of temperature field and heat transfer analysis for the piston of diesel engine with and without air cavity," *Jordan J. Mech. Ind. Eng.*, vol. 9, no. 2, pp. 139–147, 2015.
- [16] Y. Lu, X. Zhang, P. Xiang, and D. Dong, "Analysis of thermal temperature fields and thermal stress under steady temperature field of diesel engine piston," *Appl. Therm. Eng.*, vol. 113, pp. 796–812, 2017, doi: 10.1016/j.applthermaleng.2016.11.070.
- [17] F. Zhao, "Modeling and thermal-mechanical coupling analysis of piston in car engines," *Ann. Chim. Sci. des Mater.*, vol. 45, no. 1, pp. 83–92, 2021, doi: 10.18280/acsm.450111.
- [18] J. K. Sharma, R. Raj, S. Kumar, R. K. Jain, and M. Pandey, "Finite element modelling of Lanthanum Cerate (La₂Ce₂O₇) coated piston used in a diesel engine," *Case Stud. Therm. Eng.*, vol. 25, p. 100865, 2021, doi: 10.1016/j.csite.2021.100865.
- [19] Z. Qian, Y. Hu, C. Fei, Z. Shu, S. Zhu, and Y. Du, "Finite Element Analysis of Thermal and Stress Fields of Diesel Engine Piston with GZO/YSZ Dual-Ceramic Layer Thermal Barrier Coating," *Coatings*, vol. 15, no. 3, 2025, doi: 10.3390/coatings15030259.
- [20] A. Ghoujehzadeh, M. A. Mohtadi-Bonab, and D. Jahani, "Optimization and finite element analysis of an aluminum piston in the Peugeot XU7JPL3 engine for enhanced efficiency and durability," *Discov. Mech. Eng.*, vol. 4, no. 1, 2025, doi: 10.1007/s44245-025-00091-w.
- [21] Y. Du, C. Fei, Z. Qian, S. Zhu, Z. Shu, and K. Zhou, "Simulation analysis of thermal insulation performance of diesel engine piston based on PEO and La₂Zr₂O₇ thermal barrier coating," *Case Stud. Therm. Eng.*, vol. 59, no. January, p. 104460, 2024, doi: 10.1016/j.csite.2024.104460.
- [22] Z. Shu *et al.*, "Thermal Analysis of Mullite Coated Piston Used in a Diesel Engine," *Coatings*, vol. 12, no. 9, pp. 1–11, 2022, doi: 10.3390/coatings12091302.
-

- [23] Q. Jing, Y. Dong, J. Liu, H. Li, Y. Liu, and S. Zhang, "Analysis and Optimization Study of Piston in Diesel Engine Based on ABC-OED-FE Method," *Math. Probl. Eng.*, vol. 2021, 2021, doi: 10.1155/2021/3205695.
- [24] S. H. Performance, "4032 Aluminium Alloy Product Data Sheet," 2019.
- [25] U. Singh, J. Lingwal, A. Rathore, S. Sharma, and V. Kaushik, "Comparative analysis of different materials for piston and justification by simulation," *Mater. Today Proc.*, vol. 25, no. xxxx, pp. 925–930, 2019, doi: 10.1016/j.matpr.2020.03.078.
- [26] J. Mahmoudi, "Thermo-Mechanical Analysis of a Typical Vehicle Engine Using PTC-Creo," *J. Mech. Mater. Mech. Res.*, vol. 5, no. 2, pp. 1–15, 2022, doi: 10.30564/jmmmr.v5i2.4600.
- [27] A. Ahmed, M. S. Wahab, A. A. Raus, K. Kamarudin, Q. Bakhsh, and D. Ali, "Mechanical Properties, Material and Design of the Automobile Piston: An Ample Review," *Indian J. Sci. Technol.*, vol. 9, no. 36, 2016, doi: 10.17485/ijst/2016/v9i36/102155.
- [28] H. Topkaya, M. Q. Brewster, and H. Aydın, "Comprehensive Investigation of Partitioned Thermal Barrier Coating: Impact on Thermal and Mechanical Stresses, and Performance Enhancement in Diesel Engines," *Appl. Sci.*, vol. 14, p. 20, 2024.
- [29] A. International, "Properties of Wrought Aluminum and Aluminum Alloys," 2018. doi: 10.31399/asm.hb.v02.a0001060.
- [30] Z. C. Sims *et al.*, "High performance aluminum-cerium alloys for high-temperature applications," *Mater. Horizons*, vol. 4, no. 6, pp. 1070–1078, 2017, doi: 10.1039/c7mh00391a.
- [31] O. D. Inusah, J. K. Nkrumah, and V. A. Atindana, "Static and Thermal Analysis of Aluminium (413,390,384 and 332) Piston Using Finite Element Method," *Model. Numer. Simul. Mater. Sci.*, vol. 14, no. 01, pp. 1–38, 2024, doi: 10.4236/mnsms.2024.141001.
- [32] P. R. Jeyakrishnan, K. Balasubramanian, M. R. Balasubramanian, G. K. Sudharson, and S. V. Panicker, "An avant garde study on design and analysis of honey comb structured piston," *Mater. Today Proc.*, vol. 37, no. Part 2, pp. 600–607, 2020, doi: 10.1016/j.matpr.2020.05.621.
- [33] T. S. Sachit, R. V. Nandish, and Mallikarjun, "Thermal analysis of Cr2O3 coated diesel engine piston using FEA," *Mater. Today Proc.*, vol. 5, no. 2, pp. 5074–5081, 2018, doi: 10.1016/j.matpr.2017.12.086.
- [34] "Comparing Forged Pistons - 4032 Alloy Vs. 2618 Alloy - Mountune USA." <https://mountuneusa.com/blogs/technical-info/comparing-forged-pistons-4032-alloy-vs-2618-alloy?srsltid=AfmBOop-4Onpf0aGQJymp9woznRmgO823L8AjQ2VBwjFoJv3fXO9SFxE> (accessed Jul. 05, 2025).
- [35] V. Mereuta, "Static and Thermal Analysis of Piston using FEM Analysis," *Int. J. Res. Appl. Sci. Eng. Technol.*, vol. 6, no. 1, pp. 201–206, 2018, doi: 10.22214/ijraset.2018.1032.

This page is intentionally left blank